

Ultra-small moment incommensurate spin density wave order masking a ferromagnetic quantum critical point in NbFe₂ - Supplemental Material

P. G. Niklowitz,^{1,*} M. Hirschberger,² M. Lucas,¹ P. Cermak,³ A. Schneidewind,³ E. Faulhaber,⁴ J.-M. Mignot,⁵ W. J. Duncan,¹ A. Neubauer,⁶ C. Pfeleiderer,⁶ and F. M. Grosche⁷

¹Department of Physics, Royal Holloway, University of London, Egham TW20 0EX, U.K.

²Department of Physics, Princeton University, Princeton, NJ08544, U.S.A.

³Jülich Centre for Neutron Science (JCNS) at Heinz Maier-Leibnitz Zentrum (MLZ), Forschungszentrum Jülich GmbH, Lichtenbergstr. 1, 85748 Garching, Germany

⁴Heinz Maier-Leibnitz Zentrum (MLZ), Technische Universität München, Lichtenbergstr. 1, 85748 Garching, Germany

⁵Laboratoire Léon Brillouin (CEA-CNRS), CEA Saclay, F-91191 Gif-sur-Yvette, France

⁶Physik Department E21, Technische Universität München, 85748 Garching, Germany

⁷Cavendish Laboratory, University of Cambridge, Cambridge CB3 0HE, U.K.

PACS numbers:

Keywords:

SAMPLE CHARACTERISATION

We have studied three large single crystals, which are approximately 6 mm wide and between 4 and 15 mm long.

Sample A (designation OFZ12-x). In magnetic susceptibility measurements (Fig. 1) this sample shows a dis-

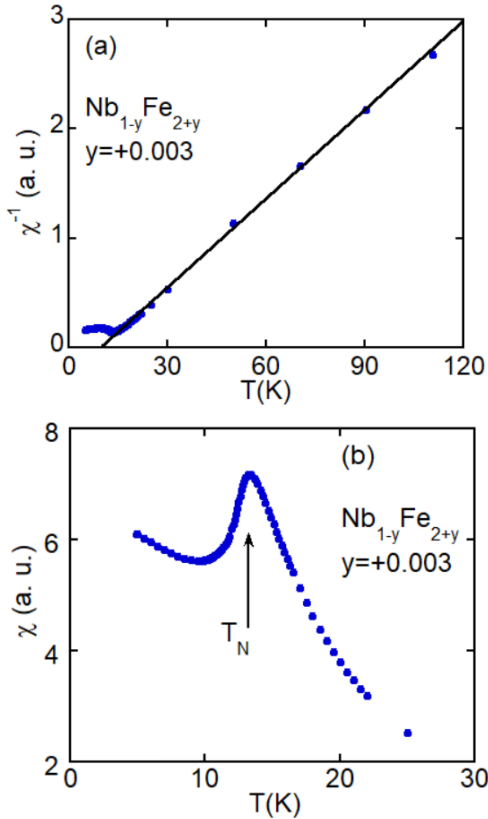


FIG. 1: T dependence of the magnetic susceptibility of Sample A. (a) shows the inverse susceptibility and (b) the low-temperature susceptibility, where $T_N = 13$ K (arrow) is observed.

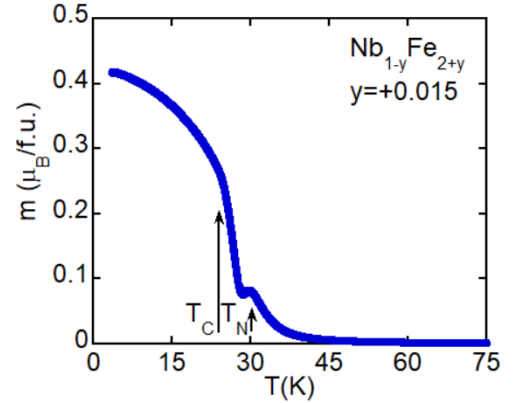


FIG. 2: T dependence of the magnetisation measured after field cooling of a piece cut off from Sample B. T_N and T_C are observed at 30 K and 24 K, respectively (arrows).

tinct peak at 13 K and no ferromagnetism down to 2 K. The peak position is close to T_N determined by neutron scattering.

Sample B (designation OFZ27.3). In our magnetisation measurements (Fig. 2) a fragment cut from Sample B shows two phase transition anomalies, at $T_C = 24$ K and $T_N = 30$ K. The onset temperatures of Sample B in neutron scattering are $T = 24.5$ K for the FM transition and $T = 32.3$ K for the SDW transition (main text Fig. 3). We note that the peak intensity for the SDW signature in neutron scattering coincides with the FM onset temperature of $T = 24.5$ K, whereas the SDW intensity vanishes at $T = 18.5$ K. Because we know from prior magnetic studies that the SDW-FM transition is first order, this overlap region of 6 K must be attributed to a distribution of sample compositions. Main text Fig. 1 shows that a variation of T_C by ± 3.0 K corresponds to a variation of composition y by ± 0.0016 . This composition variation leads, in turn, to a variation of T_N by ± 2.2 K. This causes the *bulk* neutron transition

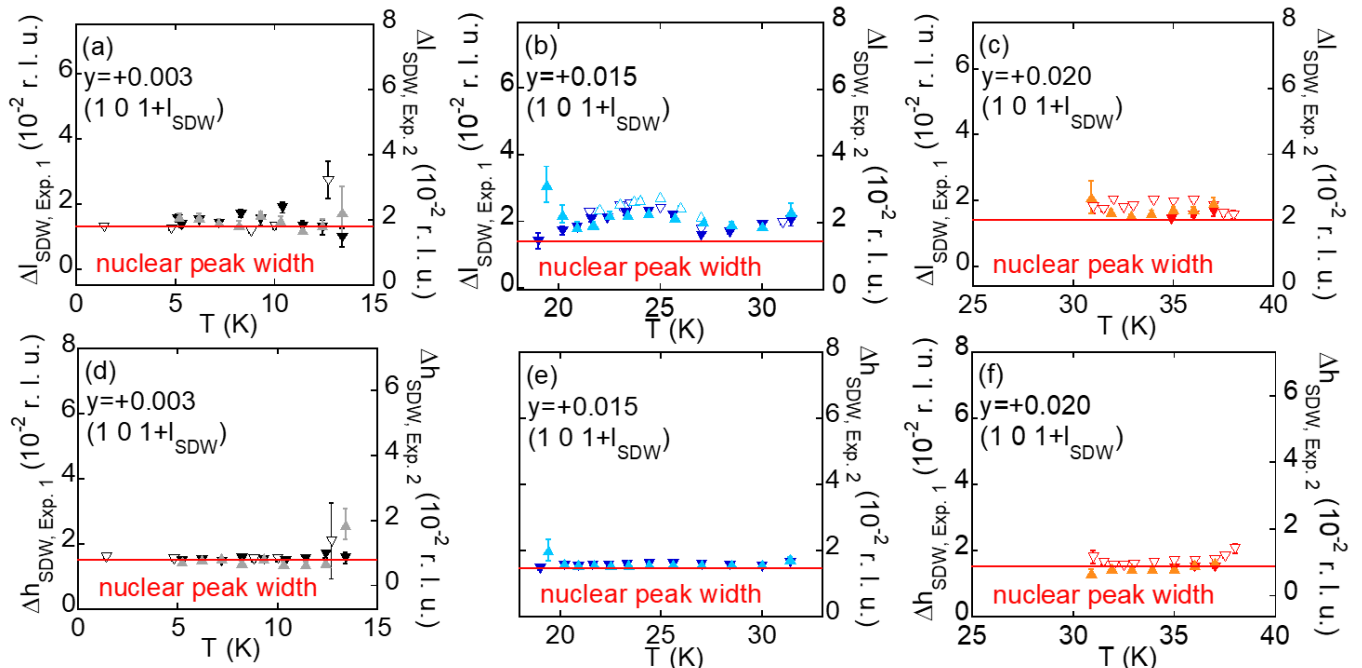


FIG. 3: Neutron diffraction at $\mathbf{Q} = (1, 0, 1+l_{\text{SDW}})$ of $\text{Nb}_{1-y}\text{Fe}_{2+y}$ samples A ($y = +0.002$), B ($y = +0.014$), and C ($y = +0.019$). The T dependence of the SDW peaks' l and h widths is shown in Figures (a)-(c) and (d)-(f), respectively. SDW peak width values are weighted average widths whenever multiple Gaussian fit functions have been used. The SDW peak widths are compared to the corresponding width values of the nearby nuclear (101) peaks, which are indicated by red lines and have been obtained by equivalent Gaussian fits.

temperatures to be about 3.0 K (2.2 K) lower than the onset temperatures for T_C (T_N), respectively, and gives $T_{C,\text{neutrons,bulk}} \approx 21.5$ K and $T_{N,\text{neutrons,bulk}} \approx 30.1$ K, in good agreement with the magnetisation data shown in Fig. 2. Moreover, neutron depolarisation measurements of Sample B have previously suggested a FM onset temperature between $T = 24$ K and $T = 26$ K (Ref. [1]) and confirmed homogeneous FM order below $T = 19$ K, where our neutron diffraction data shows that SDW order is almost fully suppressed.

Sample C (designation OFZ28.3.2.4). Prior AC susceptibility and magnetisation measurements on a fragment cut from this large crystal (Ref. [2]) show two phase transition anomalies, at $T_C = 33$ K and $T_N = 37$ K. The onset temperatures in our neutron data (main text Fig. 3) are $T = 34$ K for the FM transition and $T = 38.3$ K for the SDW transition. The SDW/FM overlap region (main text Fig. 3b) is about 3.5 K wide, suggesting that the bulk transition temperatures fall 1.8 K (1.2 K) below the onset temperatures for FM (SDW), respectively. This gives $T_{C,\text{neutrons,bulk}} \approx 32.2$ K and $T_{N,\text{neutrons,bulk}} \approx 37.1$ K, in very good agreement with the magnetic measurements in Ref. [2]. Neutron depolarisation measurements at temperatures of up to $T = 30$ K have confirmed a homogeneous FM state [1].

EXPERIMENTAL SET-UP

Neutron diffraction was carried out at two cold triple-axis spectrometers in diffraction mode: Panda operated by JCMS at the Heinz Maier-Leibnitz Zentrum (MLZ) and 4F2 at the Laboratoire Léon Brillouin (LLB). At both instruments both PG monochromator and PG analyser were set to be vertically focusing and horizontally flat. No collimation was used. Higher-order harmonics were removed from the scattered beam by a closed-cycle refrigerator cooled Be filter after the sample and monitor correction for higher order neutrons has been included in the analysis.

DATA ANALYSIS

For the analysis of the SDW Bragg reflections the shape of the fit function has been determined by the shape of the nearby nuclear (101) Bragg reflection, which is influenced by sample mosaicity and instrumental resolution. In all cases \mathbf{q} scans through (101) revealed single, double, or triple Gaussian peak shapes. The resulting nuclear peak shape has then been used to fit the SDW Bragg reflections. The SDW peak fit functions also contain a constant background contribution. In the case of Sample C the background also contains contributions from a

weak broad Gaussian centred at \mathbf{q}_{SDW} , and from a very weak Gaussian tail of the nuclear (101) Bragg reflection.

In order to obtain the T dependence of the integrated intensities of the FM Bragg reflections, the T dependence of the (102) count rates have been measured and a linear nuclear background has been subtracted.

SDW BRAGG PEAK WIDTHS

The SDW and nuclear peak widths are generally found to be very similar. The l and h widths of the SDW Bragg reflection at $\mathbf{Q} = (1, 0, 1 + l_{\text{SDW}})$ are shown in Fig. 3. The widths are compared to the corresponding width values of the nearest nuclear (101) Bragg reflection. Only in the range where \mathbf{q}_{SDW} is T dependent SDW Bragg peaks show slight broadening in the l direction corresponding to a correlation length of the order of 100 nm, which is otherwise found to be at least of the order of $1 \mu\text{m}$.

ESTIMATE OF THE FM ORDERED MOMENT

Relative estimates of the FM ordered moments are given by the ratios of the FM and nuclear (102) Bragg peak values. Absolute estimates of the FM ordered moments are then obtained by the ratio of FM and nuclear (102) Bragg peak values in Sample C at $T = 13 \text{ K}$, where the ordered moment of a piece cut off from Sample C has been independently determined by DC magnetisation measurements to be $\mu_{\text{FM}} = 0.12 \mu_{\text{B}}/(\text{Fe atom})$ [2].

ESTIMATE OF THE SDW ORDERED MOMENT

Relative estimates of the SDW ordered moments are given by the ratios of the integrated intensities of the SDW Bragg peaks at $\mathbf{Q} = (1, 0, 1 + l_{\text{SDW}})$ to the nuclear part of the (102) Bragg peak intensities. Extinction effects are not expected due to the weakness of the (102) nuclear signal. Absolute estimates of the SDW ordered moments are then obtained by the ratio of FM and nuclear (102) Bragg peak values in Sample C at $T = 13 \text{ K}$, as described in the previous section. Integrated (102) Bragg peak intensities have been obtained from the peak values at (102) and the peak widths at (101) assuming that (102) nuclear and FM signal widths are similar to measured nuclear (101) Bragg peak widths. It has also been assumed that both the ordered SDW and FM moments point along the easy c -axis. The ratio of the squares of the SDW moment μ_{s} and FM ordered moment μ_{FM} is given by the ratio of the integrated intensities of the SDW peak $I_{(101+l_{\text{SDW}})}$ and the FM peak $I_{(102),\text{FM}}$

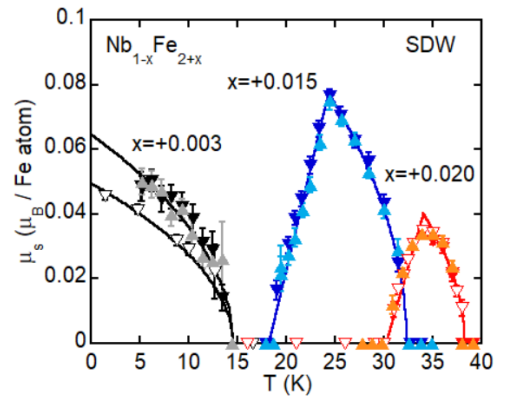


FIG. 4: T dependences of SDW ordered moments μ_{s} obtained from measurement sequences going down (downward triangles) and up (upward triangles) in T for Samples A ($y = +0.003$, black, grey), B ($y = +0.015$, dark blue, light blue), and C ($y = +0.020$, red, orange). Each sample has been investigated in two separate experiments (empty and filled symbols, respectively). Lines to the right of the maxima are fits described in the text. Lines to the left of the maxima are guides to the eye. μ_{s} values have been estimated from integrated intensities at $\mathbf{Q} = (1, 0, 1 + l_{\text{SDW}})$ and comparison with strong nuclear (101) intensities. Differences between the relative moment sizes of the different samples in this figure and in Fig. 3b of the main text are likely caused by extinction effects on the (101) intensities. Discrepancies in μ_{s} values of 25% between measurements of Sample A in the two separate experiments illustrate the uncertainty of the μ_{s} values. μ_{s} values of the two separate experiments on Sample C are in close agreement.

using the formula

$$\frac{I_{(101+l_{\text{SDW}})}}{I_{(102),\text{FM}}} = \frac{\mu_{\text{s}}^2}{\mu_{\text{FM}}^2} \frac{S_{(101+l_{\text{SDW}})}^2}{S_{(102),\text{FM}}^2} \frac{F_{(101+l_{\text{SDW}})}^2}{F_{(102),\text{FM}}^2} \frac{p_{(101+l_{\text{SDW}})}^2}{p_{(102),\text{FM}}^2}$$

with the ratio of the squares of the structure factors $S_{(101+l_{\text{SDW}})}^2/S_{(102),\text{FM}}^2 = 0.615$, the ratio of the squares of the form factors $F_{(101+l_{\text{SDW}})}^2/F_{(102),\text{FM}}^2 = 1.21$, and the ratio of the squares of the selection-rule effects $p_{(101+l_{\text{SDW}})}^2/p_{(102),\text{FM}}^2 = 1.58$. Results of different measurements of the same sample in the same experimental setup (Fig. 4) illustrate the uncertainty in the size of the observed ordered SDW moments of up to 25% from these measurements. Not all of those measurements included data at (102) and therefore in this case absolute estimates of the SDW ordered moments have been obtained by the ratios of the integrated intensities of the SDW Bragg peaks to the strong nuclear (101) Bragg peak intensities and by the ratio of FM (102) and nuclear (101) integrated Bragg peak intensities in Sample C at $T = 13 \text{ K}$.

LANDAU PARAMETERS OF TWO ORDER PARAMETER MODEL

The phase diagram can be modelled using a Landau expansion of the free energy in terms of the two order parameters M (for FM) and P (for SDW order) [3], which in zero field reduces to

$$\frac{F}{\mu_0} = \frac{a}{2}M^2 + \frac{b}{4}M^4 + \frac{\alpha}{2}P^2 + \frac{\beta}{4}P^4 + \frac{\eta}{2}P^2M^2 .$$

. Analysis of Arrott plots [3] shows that a linear temperature dependence holds for the phenomenological parameter $a = a_1(T - T_0)$ and that b is roughly T -independent, causing us likewise to approximate $\alpha = \alpha_1(T - T_N)$, and β , and η to be independent of T .

The model then has the seven free parameters a_1 , T_0 , b , α_1 , T_N , β , and η , which all depend on the excess Fe concentration y . All parameters can be calculated from the following seven y dependent experimentally obtained quantities. The phase diagram (Fig. 1 of main text) provides T_N and T_C . From magnetisation measurements [3] a_1 and b as well as $a^* := a - \alpha\eta/\beta$ and $b^* := b - \eta^2/\beta$ have been obtained for two y compositions. We can write $a^* = a_0^* + a_1^*(T_N - T)$ and obtain $a_1^* = \alpha_1\eta/\beta - a_1$. A linear y extrapolation is assumed for a_1 , b , a_1^* , and b^* . Finally, the SDW ordered moments measured in this study have been fitted with $\mu_s = c\sqrt{T_N - T}$ with c being the last required experimental quantity (Fig. 3b of main text and Fig. 4.) to fully solve the model.

For the samples of this study we have first calculated the auxiliary parameters

$$c_1 := \frac{\alpha_1\eta}{\beta} = a_1 + a_1^* ,$$

$$c_2 := \eta^2/\beta = b - b^* , \text{ and}$$

$$c_3 := \frac{\alpha_1}{\beta} = c^2 .$$

From those parameters we have then obtained

$$\eta = \frac{c_1}{c_3} ,$$

$$\beta = \frac{c_1^2}{c_2 c_3^2} , \text{ and}$$

$$\alpha_1 = \frac{c_1^2}{c_2 c_3} .$$

For Sample B and C the temperature T_0 of the masked continuous FM transition has been calculated using the condition for the SDW-FM phase transition $a^2/b = \alpha^2/\beta$, which leads to the expression

$$T_0 = T_C - \frac{c_1}{a_1} \sqrt{\frac{b}{c_2}} (T_C - T_N) .$$

For Sample A there is no T_C value within the measured T range. Therefore, T_0 has been obtained from an extrapolation of available T_0 values of the two single crystals studied with magnetisation measurements [3] and calculated T_0 values for Samples B and C of this study.

sample	A	B	C
y	0.003	0.015	0.020
$a_1(T/(\mu_B/\text{atom}))$	3.7(0.5)	4.7(0.5)	5.1(0.5)
$\alpha_1(T/(\mu_B/\text{atom}))$	5.9(1.6)	5.2(1.4)	10.2(2.8)
α_1/a_1	1.6(0.6)	1.1(0.4)	2.0(0.7)
$b(10^3 T/(\mu_B/\text{atom})^3)$	27(2)	15(2)	10(2)
$\beta(10^3 T/(\mu_B/\text{atom})^3)$	68(36)	26(14)	60(32)
β/b	2.5(1.5)	1.7(1.1)	6.0(4.4)
$\eta(10^3 T/(\mu_B/\text{atom})^3)$	59(16)	27(7)	32(9)
η/β	0.9(0.7)	1.0(0.8)	0.5(0.4)
$\eta/\sqrt{b\beta}$	1.36(0.05)	1.34(0.05)	1.31(0.05)

TABLE I: Landau parameters of the two-order parameter model for Samples A, B, and C. The dominant error is the uncertainty of the sizes of the SDW ordered moments. $\eta/\sqrt{b\beta}$ is independent of the latter uncertainty.

The Landau parameters of the two-order parameter model for Samples A, B, and C are listed in Table I.

The parameters characterising the SDW order vary slowly with composition and are of similar magnitude as those characterising the FM order: $\alpha_1/\alpha \simeq \beta/b \simeq 2 \pm 1$ and the coupling parameter $\eta \simeq \beta$. The ratio $\eta/\sqrt{b\beta} = 1.34(0.05)$.

* e-mail: philipp.niklowitz@rhul.ac.uk

- [1] A. Neubauer, Ph.D. thesis, Technische Universität München (2011).
- [2] T. D. Haynes, I. Maskery, M. W. Butchers, J. A. Duffy, J. W. Taylor, S. R. Giblin, C. Uffeld, J. Laverock, S. B. Dugdale, Y. Sakurai, et al., Phys. Rev. B **85**, 115137 (2012).
- [3] S. Friedemann, W. J. Duncan, M. Hirschberger, T. W. Bauer, R. Kuchler, A. Neubauer, M. Brando, C. Pfleiderer, and F. M. Grosche, Nature Phys. **14**, 62 (2018).